

## Synthesis and Electroluminescent Properties of OLED Green Dopants Based on BODIPY Derivatives

Quynh Pham Bao Nguyen, Hee Min Hwang, Mi-Seon Song, Hui Jeong Song,  
Gyeong Heon Kim,<sup>†</sup> Jang Hyuk Kwon,<sup>†</sup> Na Young Shim,<sup>‡</sup> and Kyu Yun Chai<sup>\*</sup>

The Division of Bio-Nanochemistry, The College of Natural Sciences, The Wonkwang University, Iksan, Chonbuk 570-749, Korea. \*E-mail: geuyoon@wonkwang.ac.kr

<sup>†</sup>Department of Information Display, Kyung Hee University, Dongdaemoon-gu, Seoul 130-701, Korea

<sup>‡</sup>Venture Building, #824, Palbokdong 2-ga, Deokjin-gu, Jeonju, Chonbuk 561-844, Korea

Received January 5 2014, Accepted January 24 2014

**Key Words :** Green dopant, BODIPY, 9-Phenylcarbazole, Triphenylamine

Organic light-emitting diodes (OLEDs) based on the small organic molecules have gained remarkable attention for display and solid-state lighting applications over the last few years due to their well-defined molecular structures, facile syntheses and modifications, and specific structure-property correlations.<sup>1,2</sup> One approach that has been used to improve the efficiency of the OLED devices in term of brightness and stability is the introducing of the highly fluorescent organic guest dopants into the host materials to obtain the full color display.<sup>3</sup> Therefore, there is still a need for the development of new dopants with good color purity, stability and high efficiency.<sup>4</sup> Difluoroboradiaza-*s*-indacene (BODIPY) represents an outstanding class of fluorophore with high quantum yield, large molar absorption coefficient, high chemical, thermal and photophysical stability.<sup>2,5-8</sup> The development of new BODIPY derivatives has become a booming of research due to their potential applications in luminescent devices, chemical sensors, biological labeling, and photovoltaic cells.<sup>9-12</sup> Major efforts have been devoted to obtain the well-designed BODIPY structures by modifying of the pyrrole core, fusing some aromatic rings to the BODIPY core, and replacing the 8-carbon atom with a nitrogen atom to form

*aza*-BODIPY. The incorporation of boron element into the  $\pi$ -conjugated framework may lead to the appearance of unique electronic and photophysical properties.<sup>13,14</sup> Recently, we have successfully explored some green dopants based on arylamine 2,3-disubstituted bithiophene derivatives for OLEDs.<sup>15</sup> In the course of our ongoing studies, herein we wish to report the novel green dopants based on BODIPY and two different arylamine moieties with good overall performance in the multilayer device (Figure 1).

In the design of the target molecules **5a–b** (Figure 1), the outstanding fluorescent BODIPY core was fused with different arylamine moieties which were expected to enhance the light emitting efficiency through the extension of the

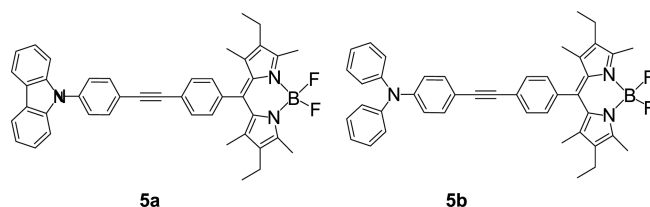
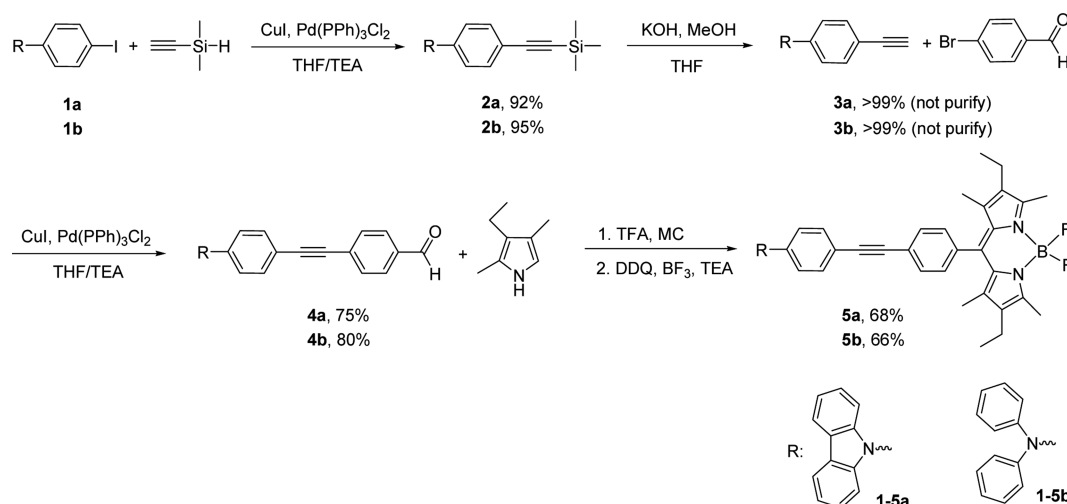


**Figure 1.** Structures of designed green dopants **5**.



**Scheme 1.** Synthesis of green dopants **5**.

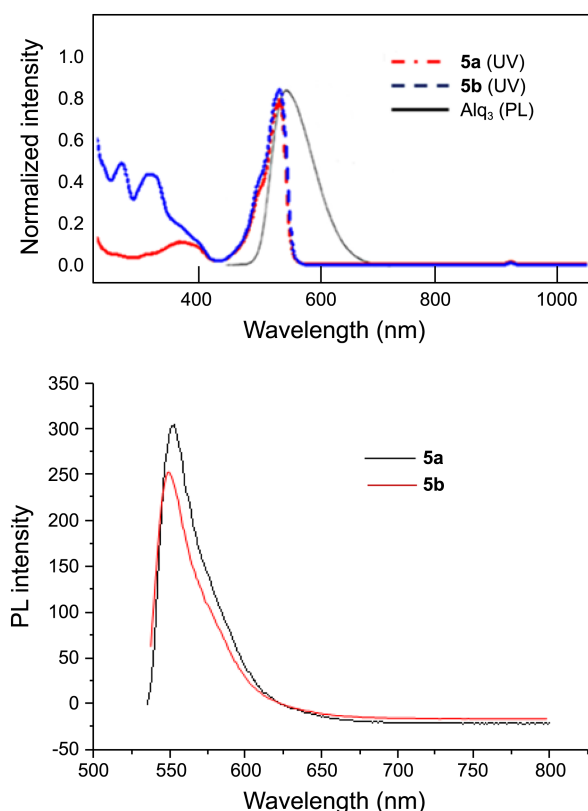


**Figure 2.** PL and UV spectra of green dopants **5**.

conjugated structures as well as to improve the charge transport properties. The syntheses of the desired compounds **5a–b** were accomplished through four steps from the commercially available arylamine iodides **1** in good yields (Scheme 1). Sonogashira cross-coupling of **1** with trimethylsilyl ethyne afforded compounds **2** which were deprotected with potassium hydroxide in methanol to give the activated **3** in excellent yields. Sonogashira cross-coupling of **3** again with 4-bromobenzaldehyde proceeded well to produce the corresponding compounds **4**. The key one-pot reactions in the syntheses of BODIPYs **5a–b** contained three processes: (i) the methane bridge formation of pyrrole with aldehydes **4** under the acid catalyst, (ii) the oxidation of the meso carbon with 2,3-dichloro-5,6-dicyanobenzoquinone (DDQ), and (iii) the complexation of  $\text{BF}_3 \cdot \text{OEt}_2$  with dipyrrole unit in the presence of triethylamine base. Finally, the desired BODIPYs **5a–b** were obtained in 68 and 66% yields, respectively.

Before the fabrication of OLED devices, the two green dopants **5a–b** were characterized by NMR, IR, UV-Vis,

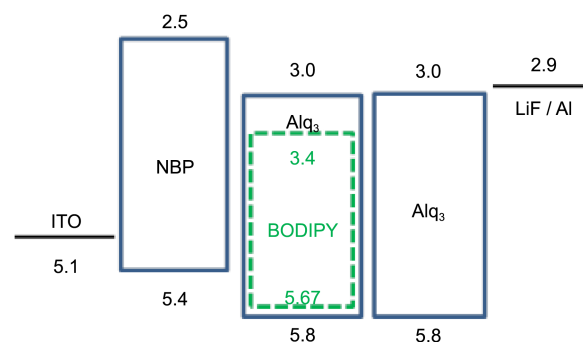


**Figure 3.** Energy levels of the OLED device.

photoluminescent (PL) spectroscopies, differential scanning calorimetry (DSC), thermogravimetric analysis (TGA) and energy levels HOMO-LUMO (Figure 2 and Table 1). The optical properties of the compounds **5a–b** were determined by UV-Vis and PL spectroscopies in dichloromethane. The UV-Vis absorption peaks of **5a–b** were observed at 526 and 524 nm, respectively while the emission peaks were observed in the green region at 552 and 551 nm, respectively. As seen in Figure 2, the absorption spectra of **5a–b** overlapped with the emission spectra of the common tris-(8-hydroxyquinoline) aluminum ( $\text{Alq}_3$ ), a key green-light emitting and electron transport material for OLEDs. That implied **5a–b** could accept the energy transfer from  $\text{Alq}_3$ . The electrochemical properties of **5a–b** were investigated by the cyclic voltammetric measurements. The energy of the highest occupied molecular orbital (HOMO) and that of the lowest unoccupied molecular orbital (LUMO) of the green dopants **5a–b** were determined and compared with those of *N,N'*-di(naphthalen-1-yl)-*N,N'*-diphenyl-benzidine (NPB), one of the most widely used hole-transport material in OLEDs (Table 1). The HOMO/LUMO energy levels of compounds **5a–b** were 5.67/3.40 and 5.69/3.42 eV, respectively and their calculated HOMO-LUMO energy gaps ( $E_g$ ) were the same at 2.27 eV. It is necessary to have HOMO and LUMO levels of the guest dopant suitably aligned with the HOMO and LUMO of the host emitter for good device operation. As seen in Table 1 and Figure 3, compounds **5a–b** satisfied the energy level conditions to be suitable as dopants for application in OLEDs. In addition, the thermal properties of **5a–b** were also examined by DSC and TGA analysis. Both compounds showed good thermal stability with the glass transition temperature ( $T_g$ ) of 243 and 260 °C (Table 1).

The strong PL emission, tunable energy levels, enhanced thermal properties, and excellent solubility of **5a–b** encour-

**Table 1.** Photophysical properties of green dopants **5**

Compound	$T_g$ (°C)	UV $\lambda_{\text{max}}$ (nm) <sup>a</sup>	PL $\lambda_{\text{max}}$ (nm) <sup>a</sup>	$E_{\text{ox}}$ (eV) <sup>c</sup>	HOMO (eV) <sup>d</sup>	LUMO (eV) <sup>d</sup>	$E_g$ (eV)
NPB	— <sup>b</sup>	— <sup>b</sup>	— <sup>b</sup>	0.55	5.40	2.50	2.90
<b>5a</b>	243	526	552	0.82	5.67	3.40	2.27
<b>5b</b>	260	524	551	0.84	5.69	3.42	2.27

<sup>a</sup>In dichloromethane (*ca.*  $1 \times 10^{-6}$  M). <sup>b</sup>Not determined. <sup>c</sup>Oxidation potential relative to Ag/AgCl electrode. <sup>d</sup>HOMO = ( $E_{\text{ox}} + 4.85$ ) eV; LUMO = (HOMO –  $E_g$ ) eV.

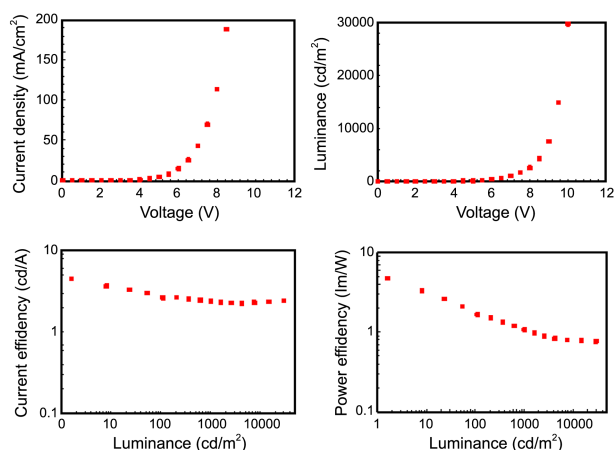


**Figure 4.** *J-V-L* and efficiency-*L* characteristics of fabricated OLED device based on BODIPY **5a**.

aged us to fabricate them in the OLED devices. As seen in Figure 2 and Table 1, these green dopants have the similar photophysical characteristics. Therefore, a standard OLED device was fabricated with the configuration of ITO/NPB (500 Å)/3 wt % of BODIPY **5a** in Alq<sub>3</sub> (200 Å)/Alq<sub>3</sub> (500 Å)/LiF (15 Å)/Al (1000 Å) to investigate their electro-luminescent properties. The characteristics of the device were shown in Figures 4-5 and Table 2. A yellowish green color (CIE = 0.40, 0.57) with a maximum emission peak at 550 nm was emitted. The device exhibited good overall performance with low turn on voltage of 3.0 V and 7.0 V driving voltage at 1,000 cd/m<sup>2</sup>. Maximum brightness, current efficiency, power efficiency and external quantum efficiency (EQE) of 30,000 cd/m<sup>2</sup> (at 10 V), 4.32 cd/A, 5.43 lm/W and 0.89% are observed, respectively. The EL spectra of fabricated **5a** device are shown in Figure 5. This device exhibited a maximum emission peak at 551 nm with shoulder peak at 450-500 nm. This shoulder peak is originated by weak NPB emission due to the charge unbalance in the device.<sup>18</sup> Observed EL spectrum has 2 nm red shifted and its spectrum widens some amount compared with that of **5a** PL. In general such behavior is originated by van der Waals inter-

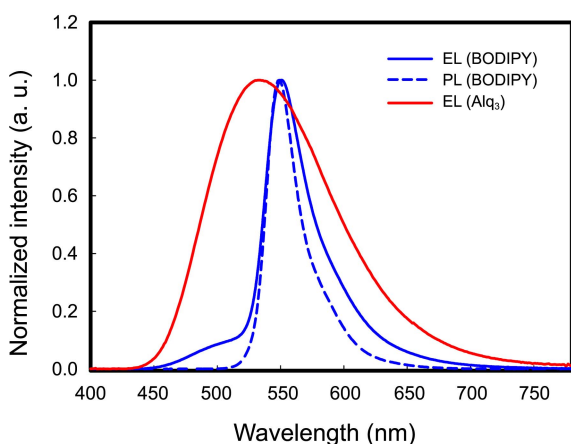


**Figure 5.** The EL, PL spectrum of fabricated OLED device based on BODIPY **5a** and Alq<sub>3</sub> (at 1,000 cd/m<sup>2</sup>).

**Table 2.** Characteristics of the OLED device based on BODIPY **5a**

Characteristics	Device	Data with 3 wt % BODIPY dopant <b>5a</b>
Turn-on voltage (at 1 cd/m <sup>2</sup> )		3.0 V
Driving voltage (at 1,000 cd/m <sup>2</sup> )		7.0 V
Efficiency (at 1,000 cd/m <sup>2</sup> )		2.38 cd/A; 1.07 lm/W
Max. efficiency		4.32 cd/A; 5.43 lm/W
Max. brightness		30,000 cd/m <sup>2</sup>
CIE color coordinate		(0.40, 0.57)
λ <sub>max</sub> (at 1,000 cd/m <sup>2</sup> )		550 nm

action of molecules in the solid film. In our spectrum, Alq<sub>3</sub> emission may contribute if energy transfer is incomplete. As shown in Figure 5, Alq<sub>3</sub> spectrum is very broad while our observed spectrum is very narrow. This indicates that energy transfer from Alq<sub>3</sub> to **5a** is efficient and there is almost no emission from Alq<sub>3</sub>.

In summary, the novel green dopants based on BODIPY and two different arylamine moieties, namely 9-phenyl-carbazole and triphenylamine have been successfully synthesized and characterized. Their photophysical properties were similar and found to be suitable for green dopants. The OLED device with the structure of ITO/NPB/BODIPY **5a** (3 wt % in Alq<sub>3</sub>)/Alq<sub>3</sub>/LiF/Al showed good performance with low turn on voltage (3.0 V), green emission (CIE = 0.40, 0.57), maximum brightness, current efficiency and power efficiency of 30,000 cd/m<sup>2</sup>, 4.32 cd/A, and 5.43 lm/W, respectively.

## Experimental

**General Procedures.** All reagents and solvents were obtained from commercial suppliers (Aldrich and TCI Chem. Co., Seoul, Korea) and were used without further purification. <sup>1</sup>H and <sup>13</sup>C NMR spectra were recorded on a JEON JNM-ECP FT-NMR spectrometer operating at 500 and 125 MHz, respectively. IR spectra were measured on a Shimadzu Prestige-21 FT-IR spectrophotometer. The samples were prepared as a KBr pellet and scanned against a blank KBr pellet background at a wave number ranging from 4000 to 400 cm<sup>-1</sup>. UV-vis absorption spectra were recorded on a Scinco S-3100 spectrophotometer while photoluminescence (PL) spectra were measured on a CARY Eclipse Varian fluorescence spectrophotometer. The HOMO levels were calculated from the oxidation potentials, while the LUMO levels were calculated based on the HOMO levels and the lowest-energy absorption edges of the UV-vis absorption spectra. Thermal gravimetric analysis (TGA) was conducted on a TG 209F1 (NET-ZSCH) thermal analysis system under a heating rate of 20 °Cmin<sup>-1</sup>.

**Synthesis.** Compounds **2**, **3** and **4** were known and synthesized by the following the previously reported methods in the literatures.<sup>16,17</sup>

**Typical Procedure for Synthesis of Compounds (5).** To a deoxygenated solution of aldehydes **4** (0.2 g, 0.539 mmol)

and 3-ethyl-2,4-dimethyl-1*H*-pyrrole (0.15 mL, 1.304 mmol) in dichloromethane (10 mL) was added a catalytic amount of trifluoroacetic acid (3 drops). The reaction mixtures were stirred under nitrogen atmosphere at room temperature for 10 h. The resulting solution were treated with 2,3-dichloro-5,6-dicyano-1,4-benzoquinone (0.12 g, 0.539 mmol) and stirred for 3 h. Then triethylamine (10 mL) and boron trifluoride diethyletherate (10 mL) were added. The reaction mixtures were stirred at room temperature for 10 h. After washing with deionized water, the organic phases were separated, dried over magnesium sulfate, filtered, and concentrated. The residues were subjected to flash column chromatography to give the requisite products **5**.

**2,6-Diethyl-4,4-difluoro-1,3,5,7-tetramethyl-8-[4-(2-(4-ethynyl-phenyl)-9*H*-carbazole)phenyl]-4-bora-3a,4a-diazas-indacene (5a).** Yield: 68%; red solid; mp 257-259 °C; FT-IR (KBr pellet):  $\nu_{\max}$  1420  $\text{cm}^{-1}$  (boron);  $^1\text{H}$  NMR (500 MHz,  $\text{CDCl}_3$ )  $\delta$  8.15 (d,  $J = 8.3$  Hz, 2H), 7.79 (d,  $J = 8.3$  Hz, 2H), 7.71 (d,  $J = 8.3$  Hz, 2H), 7.60 (d,  $J = 8.3$  Hz, 2H), 7.44 (m, 4H), 7.32 (m, 4H), 2.54 (s, 6H), 2.33 (q,  $J_1 = 7.3$  Hz,  $J_2 = 14.7$  Hz, 4H), 1.36 (s, 6H), 1.00 (t,  $J = 7.3$  Hz, 6H);  $^{13}\text{C}$  NMR (125 MHz,  $\text{CDCl}_3$ )  $\delta$  154.2, 140.6, 139.2, 138.3, 138.0, 136.2, 133.3, 133.1, 132.4, 130.6, 129.6, 128.7, 127.0, 126.2, 123.7, 121.9, 120.5, 120.4, 109.8, 90.0, 89.8, 17.2, 14.7, 12.7, 12.0.

**2,6-Diethyl-4,4-difluoro-1,3,5,7-tetramethyl-8-[4-(2-(4-ethynyl-*N,N*-diphenylaniline)phenyl)-4-bora-3a,4a-diazas-indacene (5b).** Yield: 66%; red solid; mp 261-262 °C; FT-IR (KBr pellet):  $\nu_{\max}$  1405  $\text{cm}^{-1}$  (boron);  $^1\text{H}$  NMR (500 MHz,  $\text{CDCl}_3$ )  $\delta$  8.18 (d,  $J = 8.3$  Hz, 2H), 7.80 (d,  $J = 8.7$  Hz, 2H), 7.70 (d,  $J = 8.3$  Hz, 2H), 7.61 (d,  $J = 8.7$  Hz, 2H), 7.45 (m, 5H), 7.29 (m, 5H), 2.60 (s, 6H), 2.31 (q,  $J_1 = 7.4$  Hz,  $J_2 = 14.7$  Hz, 4H), 1.39 (s, 6H), 1.16 (t,  $J = 7.4$  Hz, 6H);  $^{13}\text{C}$  NMR (125 MHz,  $\text{CDCl}_3$ )  $\delta$  154.2, 140.6, 138.3, 138.0, 136.2, 133.3, 132.6, 130.6, 128.7, 127.0, 126.2, 123.7, 120.5, 120.4, 109.8, 31.7, 22.8, 17.4, 17.2, 14.7, 14.2, 12.7, 12.0.

**OLED Fabrication and Characterization.** Glass substrate covered with indium tin oxide (ITO having a sheet resistance of  $10 \Omega/\text{m}^2$ ) was cleaned in ultrasonic baths containing acetone and 2-propanol, rinsed in deionized water. The substrate dried under a stream of nitrogen and subjected to a UV-ozone treatment. All organic and cathode metal layers were deposited by vacuum deposition technique under a pressure of  $\sim 1 \times 10^{-7}$  Torr. The deposition rate of organic layers was about 0.5 Å/s. Then, LiF and Al were deposited in another vacuum deposition system without

breaking vacuum. Deposition rates of LiF and Al were 0.1 Å/s, 5 Å/s, respectively. After deposition, the device was encapsulated in ambient nitrogen immediately. Current density-voltage ( $J$ - $V$ ) and luminance-voltage ( $L$ - $V$ ) characteristics of device were measured by using a Keithley 2635A Source Meter Unit (SMU) and Konica Minolta CS-100A. Electroluminescence (EL) spectra and CIE color coordinate were obtained using a Konica Minolta CS-2000 spectroradiometer.

**Acknowledgments.** This work was financially supported by the Ministry of Education, Science Technology (MEST) and Korea Industrial Technology Foundation (KOTEF) through the Human Training Project for Regional Innovation.

## References

- Shirota, Y. *J. Mater. Chem.* **2000**, *10*, 1.
- Zhou, Y.; Kim, J. W.; Nandhakumar, R.; Kim, M. J.; Cho, E.; Kim, Y. S.; Jang, Y. H.; Lee, C.; Han, S.; Kim, K. M.; Kim, J.-J.; Yoon, J. *Chem. Commun.* **2010**, *46*, 6512.
- Hung, L. S.; Chen, C. H. *Mat. Sci. Eng. R* **2002**, *39*, 143.
- Choi, K.; Lee, C.; Lee, K. H.; Park, S. J.; Son, S. U.; Chung, Y. K.; Hong, J.-I. *Bull. Korean Chem. Soc.* **2006**, *27*, 1549.
- Fu, G.-L.; Pan, H.; Zhao, Y.-H.; Zhao, C.-H. *Org. Biomol. Chem.* **2011**, *9*, 8141.
- Bonardi, L.; Kanaan, H.; Camerel, F.; Jolinat, P.; Retailleau, P.; Ziessel, R. *Adv. Funct. Mater.* **2008**, *18*, 401.
- Hewavitharanage, P.; Nzeata, P.; Wiggins, J. *Eur. J. Chem.* **2012**, *3*, 13.
- Uppal, T.; Hu, X.; Fronczek, F. R.; Maschek, S.; Bobadova-Parvanova, P.; Vicente, M. G. H. *Chem. Eur. J.* **2012**, *18*, 3893.
- Jiao, C.; Huang, K.-W.; Wu, J. *Org. Lett.* **2011**, *13*, 632.
- Hayashi, Y.; Obata, N.; Tamaru, M.; Yamaguchi, S.; Matsuo, Y.; Saeki, A.; Seki, S.; Kureishi, Y.; Saito, S.; Yamaguchi, S.; Shinokubo, H. *Org. Lett.* **2012**, *14*, 866.
- Krumova, K.; Cosa, G. *J. Am. Chem. Soc.* **2010**, *132*, 17560.
- Ortiz, M. J.; Garcia-Moreno, I.; Agarrabeitia, A. R.; Duran-Sampedro, G.; Costela, A.; Sastre, R.; Arbeloa, F. L.; Prieto, J. B.; Arbeloa, I. L. *Phys. Chem. Chem. Phys.* **2010**, *12*, 7804.
- Ulrich, G.; Ziessel, R.; Haefele, A. *J. Org. Chem.* **2012**, *77*, 4298.
- Ulrich, G.; Ziessel, R.; Harriman, A. *Angew. Chem. Int. Ed.* **2008**, *47*, 1184.
- Song, M.-S.; Nguyen, Q. P. B.; Song, C.-H.; Lee, D.; Chai, K. Y. *Molecules* **2013**, *18*, 14033.
- Vicente, J.; Gil-Rubio, J.; Zhou, G.; Bolink, H. J.; Arias-Pardilla, J. *Journal of Polymer Science: Part A: Polymer Chemistry* **2010**, *48*, 3744.
- Teng, C.; Yang, X.; Yang, C.; Tian, H.; Li, S.; Wang, X.; Hagfeldt, A.; Sun, L. *J. Phys. Chem. C* **2010**, *114*, 11305.
- Kang, J.-W.; Lee, S.-H.; Park, H.-D.; Jeong, W.-I.; Yoo, K.-M.; Park, Y.-S.; Kim, J.-J. *Appl. Phys. Lett.* **2007**, *90*, 223508.